JOURNAL OF GEOPHYSICAL RESEARCH, VOL. 103, NO. E9, PAGES 20,001–20,010, AUGUST 30, 1998

Galileo direction finding of Jovian radio emissions

J. D. Menietti, D. A. Gurnett, W. S. Kurth, J. B. Groene, and L. J. Granroth
Department of Physics and Astronomy, University of Iowa, Iowa City

Abstract. The Galileo spacecraft, in orbit about Jupiter, has observed distinct spin modulation of plasma wave emissions near the Ganymede (G1 and G2) encounters in the frequency range from about 100 kHz to approximately 6 MHz. Assuming circularly polarized, transverse electromagnetic radiation, we have used the spin modulation of the sweep-frequency receivers of the electric dipole antenna over many spins to estimate the source location in the spin plane of the spacecraft. Hectometric (HOM) and decametric (DAM) emission is observed by Galileo as a general and continuous background with frequent bursts that last tens of minutes and can be separated by minutes or hours. We have analyzed HOM and DAM emissions observed near Jupiter just after the G1 and G2 encounters, including two HOM/DAM "arc" signatures observed after the G2 encounter. These latter appear to be low-frequency extensions of DAM arcs, with source regions along either the Io or the Ganymede flux tube. While the uncertainties associated with the data analysis do not allow a precise source location, the HOM/DAM emission observed near the G1 and G2 encounters is consistent with a gyroresonant source region, but it is necessary to require refraction due to the Io torus to understand the results. To explain emission from apparent source regions above a gyroresonant source region, wave refraction from asymmetries in the Io plasma torus that extend along magnetic field lines is postulated. Alternatively, if such torus density asymmetries do not exist, emission with sources above a gyroresonant source region would require another free-energy source such as energetic plasma beams in the presence of density gradients or temperature anisotropies.

1. Introduction

Data returned by the Galileo spacecraft in orbit around Jupiter since December 1995 have continued to reveal remarkable new facts about the magnetosphere of the giant planet [cf. *Gurnett et al.*, 1996]. The plasma wave instrument has detected a magnetosphere about Ganymede and has been continuously returning data from Jupiter in the frequency range from 5.6 Hz to 5.6 MHz. Direction finding using spin modulation of radio wave data has been conducted by numerous terrestrial satellites [cf. *Fainberg et al.*, 1972; *Kurth et al.*, 1975; *Morgan and Gurnett*, 1991] and more recently using multiple antenna correlations from interplanetary probes [cf. *Reiner et al.*, 1993a, b; *Ladreiter et al.*, 1994]. *Kurth et al.* [1997] used occultation of radio emission observed by Galileo near the first Ganymede flyby to determine possible source regions of hectometric (HOM) emission. Their results indicate sources for the event high above the northern hemisphere, perhaps along the Ganymede or Europa flux tube. *Menietti et al.* [1998] have recently reported initial results of Galileo direction finding of HOM emissions observed near Io. Data from the Unified Radio and Plasma Wave (URAP) experiment on the Ulysses spacecraft were used to produce the first direction-finding studies of radio emissions from Jupiter using an instrument designed in part for this purpose. These studies were limited by the instrument to frequencies less than 1 MHz, however. The HOM frequency range exists in the approximate frequency range 200 kHz $< f <$ 2 MHz, whereas the decametric (DAM) frequency range extends approximately from 1 MHz $< f <$ 40 MHz [cf. *Carr et al.*, 1983; *Ladreiter and Leblanc*, 1991]. The HOM emissions are now believed to have a source either in the auroral region at $L > 6$ [cf. *Ladreiter et al.*, 1994] or near the foot of the magnetic field lines located in the range $3 < L < 10$ [*Reiner et al.*, 1993a, b; *Menietti and Reiner*, 1996].

In this paper we analyze some of the radio emission data returned by Galileo during the first two Ganymede flybys (G1 and G2). We restrict ourselves to observations obtained from the plasma wave high-frequency receiver (101 kHz $< f <$ 5.6 MHz) and thus to emissions that exist in the HOM and lower DAM frequency range. We will show that direction finding can be used to determine approximate source locations of the radio emissions and indicates a very dynamic Jovian magnetospheric environment. The results are consistent with gyroresonant source regions at the foot of the magnetic field lines, the most common theory to explain the HOM and DAM emission, only if significant refraction due to the Io torus is considered.

Paper number 97JE03555.
0148-0227/98/97JE-03555$09.00

2. Instrumentation

The plasma wave receiver on board Galileo consists of four different sweep-frequency receivers that cover the frequency range from 5.6 Hz to 5.6 MHz for electric fields and 5.6 Hz to 160 kHz for magnetic fields. For this study, only electric field data obtained by the high-frequency receiver (HFR) will be analyzed, covering the frequency range from about 101 kHz to 5.6 MHz. A single electric dipole antenna with a tip-to-tip length of 6.6 m is connected to each electric receiver. A complete set of electric field measurements is obtained every 18.67 s, with a frequency resolution of about 10% [cf. *Gurnett et al.*, 1992]. Figure 1 shows the spacecraft and orientation of the antenna relative to the spacecraft axes.

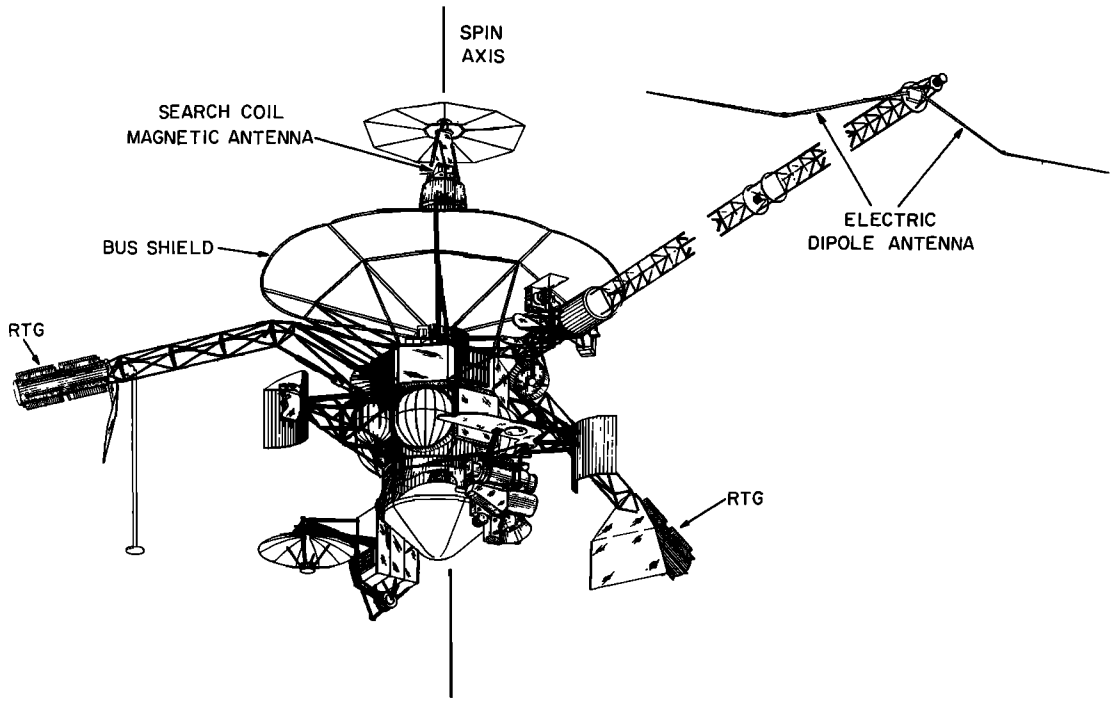

Figure 1. Galileo spacecraft showing the location and orientation of the PWS dipole antenna.

3. Direction-Finding Technique and Observations

3.1. G1 and G2 Observations

Galileo has a single electric dipole antenna along the spacecraft x axis (see Figure 1). A freely propagating, circularly polarized electromagnetic wave will be received with maximum intensity if the antenna is perpendicular to the wave vector of the incoming wave. This allows a determination of the direction to the source region in the spin plane of the spacecraft (the spin plane is always nearly perpendicular to the Jovicentric solar ecliptic (JSE) x-y plane). Information perpendicular to this plane is possible using the modulation index [*Fainberg et al.*, 1972; *Morgan and Gurnett*, 1991] if the unmodulated background signal level can be determined. The spacecraft will be in a good orientation for direction finding if the spacecraft spin axis is perpendicular to the source direction. Since the spacecraft spin axis points essentially at the Earth, Galileo was in a favorable position to see spin modulation near days 180 and 251 of 1996, just after the Ganymede flybys, G1 and G2, respectively. For these periods of time, wave amplitude modulation is often observed on a frequency-versus-time spectrogram, as in Plate 1. The modulation of the wave intensity is produced by a "beating" of the plasma wave instrument (PWS) frequency cycling period (18.67 s) against the spin period of the spacecraft (~19.0 s). In this work we assume the radio emission is not elliptically polarized, which is a good assumption for Jovian HOM emission [cf. *Reiner et al.*, 1993b, 1995]. Thus the modulation disappears if the source signal strength decreases or if the spacecraft orientation relative to the source is not favorable. In Plate 1 the modulation is seen in the kilometric and hectometric frequency range ($f > 100$ kHz) for times greater than about 0430 on day 180.

Let us assume a discrete radio emission source with constant power and location relative to Jupiter. If this source lies relatively close to the spin plane of a rotating satellite and dipole antenna, the instrument should measure power as a function of time that varies smoothly with a peak intensity when the antenna is perpendicular to the wave propagation vector. Difficulties with the technique are many in practice because the spacecraft is moving and the source regions vary in location, frequency, and amplitude with time. A plot of the spectral density versus time for about a 2.5-hour period is shown in Figure 2 at a frequency of 806 kHz. It is clear that not all of the peaks show a smooth, symmetric shape. Figure 3 is a plot of the data number (proportional to the logarithm of the electric field intensity) versus spin phase for a 70-min period of time. The curve has a period of π instead of 2π because the spacecraft antenna is properly oriented for optimum reception twice each spin period. We have performed a least squares fit of this data

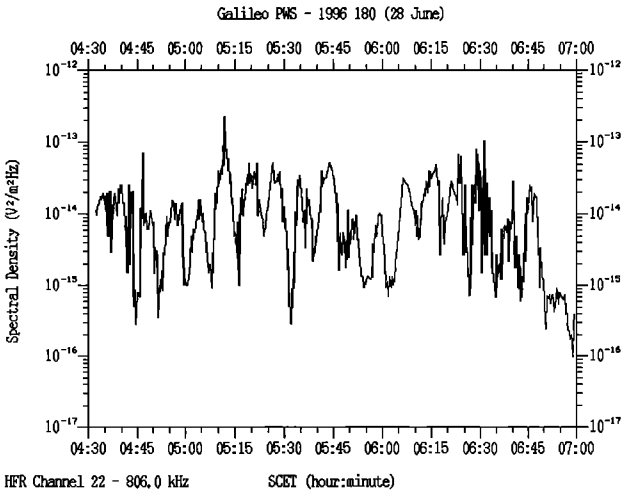

Figure 2. Electric field intensity versus time at a frequency of 806 kHz indicating the spin modulation (sinusoidal curve).

to the functional form $A + B \cos(2\phi - d)$, where ϕ is the spin angle and $d/2$ is the direction to the source in the spin plane of the satellite. The data of Figure 3 yield a look direction of $-4.2°$ (the direction of Jupiter's center is 0°). This spin plane direction is shown in Figure 4a projected into the dawn-dusk or JSE y-z plane at t = 0600 UT. Also shown on the plot are the magnetic shells for $L = 6$ (Io flux tube) and $L = 10$ and the locus of points for a right-hand extraordinary (RX) cutoff frequency of 806 kHz. A gyroresonant source should lie somewhere on this surface. For this frequency the apparent source region lies at a latitude that is lower than that which is consistent with a gyroresonant source assuming straight-line propagation. Owing to the scatter of the data points, we estimate the error of this look direction to be ±6°. The estimate of the statistical error was obtained by varying the phase angle until χ^2 changed by an amount corresponding to one standard deviation. During the time of observation (70 min) a source located along a magnetic field line would have rotated in longitude by about 42°. For directional information out of the spin plane, we have calculated the modulation index defined as $M = B/A$, which essentially is a measure of the depth of the nulls (valleys) of the modulated signal. To determine the index, it is necessary to make assumptions about the nature of the source and the background unmodulated signal. If we assume that the source is a point source out of the spin plane, it can be shown that

$$\cos\theta = |[2M/(1 + M)]|$$

where θ is the angle measured to the source away from the spin plane. We estimate the unmodulated background level by calculating the average of the highest and lowest signal strengths observed near the nulls (valleys) of Figure 3, to obtain $\theta \sim 20°$. In Figure 4b we show the spacecraft orbit and spin plane projected into the JSE x-y plane. The dashed lines indicate the extent of the source region projected into this plane. The

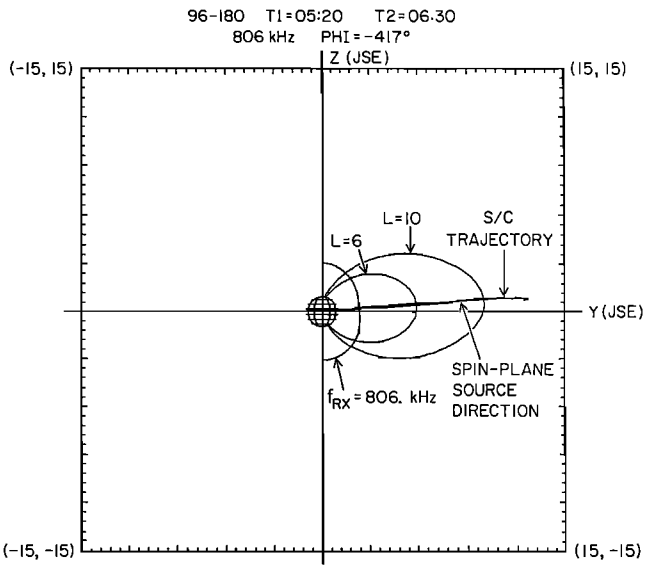

Figure 4a. Direction to the apparent source region projected into the dawn-dusk or JSE y-z plane. The direction is determined from the data of Figure 3 (806 kHz). Included in the figure are the magnetic L shells for $L = 6$ and 10, and the locus of points for the RX cutoff at $f = 806$ kHz. A gyroresonant source should lie on this surface.

direction to the source indicated in Figure 4 does not account for refractive effects of the plasma torus, which should be more pronounced at the lower frequencies. In fact, the refraction could be much larger than the statistical errors, as is discussed in section 4.

Since refractive effects are smaller at higher frequencies, we have performed the same analysis at a frequency of 4.838 MHz. A plot of the data distributed with respect to spin phase and a projection of the emission spin plane direction into the JSE y-z plane are shown in Figures 5a and 5b, respectively. We

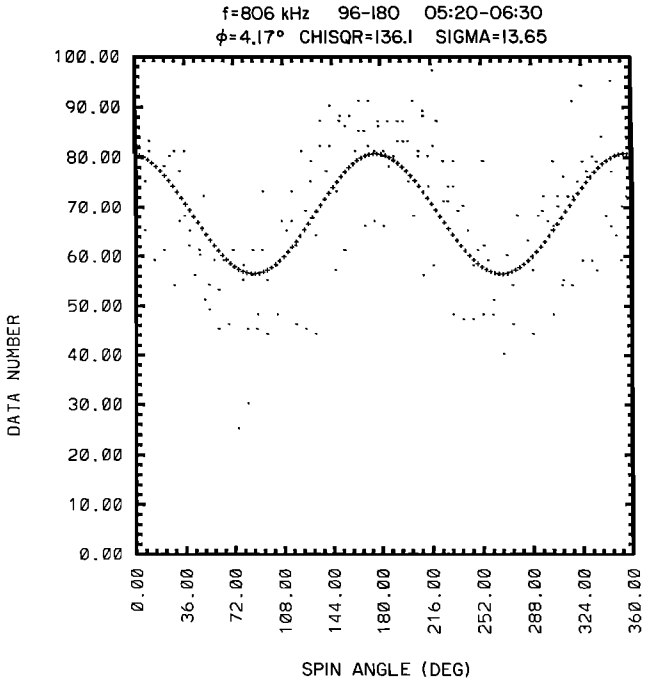

Figure 3. Wave amplitude (data number) versus spin phase for $0520 < t < 0630$ at a frequency of 806.0 kHz.

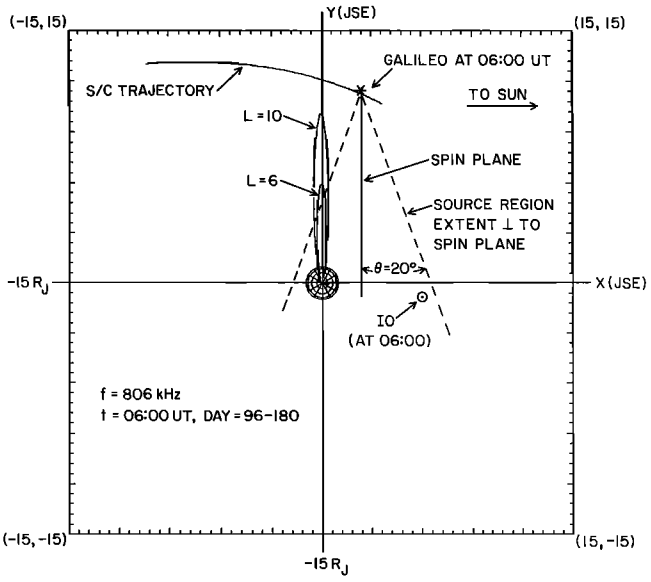

Figure 4b. Spacecraft orbit and spin plane projected into the JSE x-y plane at t = 0600 UT of day 96/180. An estimate of the extent of the source region in this plane is indicated by the dashed lines.

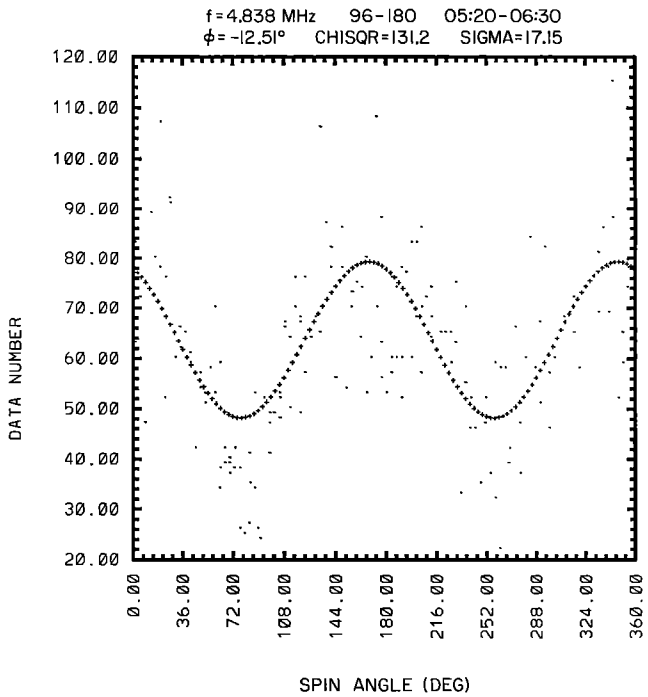

Figure 5a. Wave amplitude (data number) versus spin phase for $0520 < t < 0630$ on day 180 of 1996 at a frequency of 4.838 MHz.

believe the statistical error to be less than ±6°. The apparent source region determined from the analysis is at a higher latitude, closer to the gyroresonant source region for $f = 4.8$ MHz. Refraction due to the Io torus at this frequency will be less than that at 806 kHz, but could be as large as or larger than the statistical errors. The modulation index for this frequency indicates a source region extent perpendicular to the spin plane of the $\theta < 15°$ (not shown), measured in the JSE x-y plane.

Strong spin modulation of the wave signal was also observed on days 251 and 252 of 1996, shortly after the G2 flyby. In Plate 2 we display the color frequency-versus-time spectrograms during this time period. In this color plate the spin modulation is clearly visible, particularly in the more intense red and yellow areas of the plots. Also indicated on the plots are "holes" in the low-frequency HOM emission centered at about day 251 at 1550 and 2100 and on day 252 near 0315. We believe these holes correspond to times when the Io torus occults the low-frequency HOM emission up to about 800 kHz, consistent with the Io torus densities reported by *Gurnett et al.* [1996]. These holes occur centered at times when the spacecraft is near the magnetic equator. Two other gaps occurring on day 252 centered near 0540 and 0730 do not occur near a magnetic latitude of zero and thus may result from temporal effects or azimuthal asymmetries in the Io torus.

Analysis of the data at a frequency of 5.242 MHz is displayed in Figures 6 (data number versus rotation phase) and 7 (spin-plane source direction projected into the JSE y-z plane) for two different time intervals on this day: 1845–1945 and 2030–2130. For the earlier time period, the apparent emission direction is consistent with a gyroresonant source near Jupiter (within the statistical error of about ±6°). However, for the second time interval the apparent propagation direction is at a higher latitude, presumably not consistent with a gyroresonant source as if we assume straight-line propagation. We consider refractive effects in section 4. The statistical error in this case is also about ±6. Estimates of the unmodulated background emission are used to calculate the modulation index for these data. For the earlier time period (Figures 6a and 7a), we calculate the extent of the source region perpendicular to the spin plane to be $\theta < 18°$, whereas for the later time (Figures 6b and 7b), we obtain $\theta < 14°$. These angles are measured in the JSE x-y plane relative to the spin-plane direction (see Figure 7c).

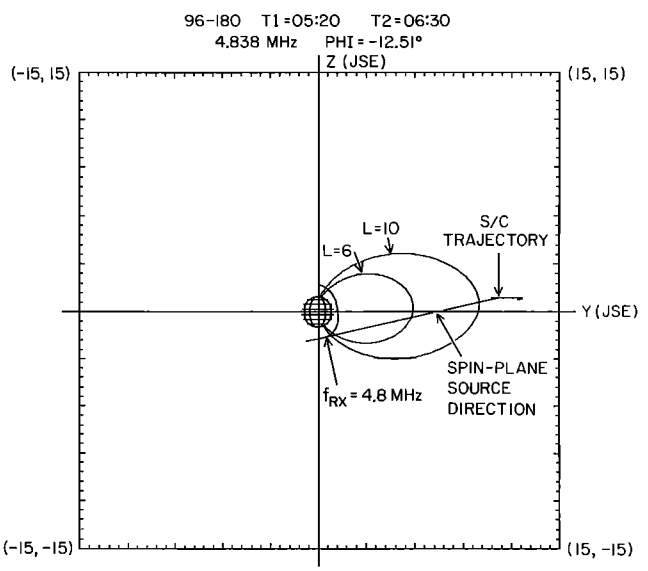

Figure 5b. Direction to the apparent source region projected into the JSE y-z plane. The direction is determined from the data of Figure 5a.

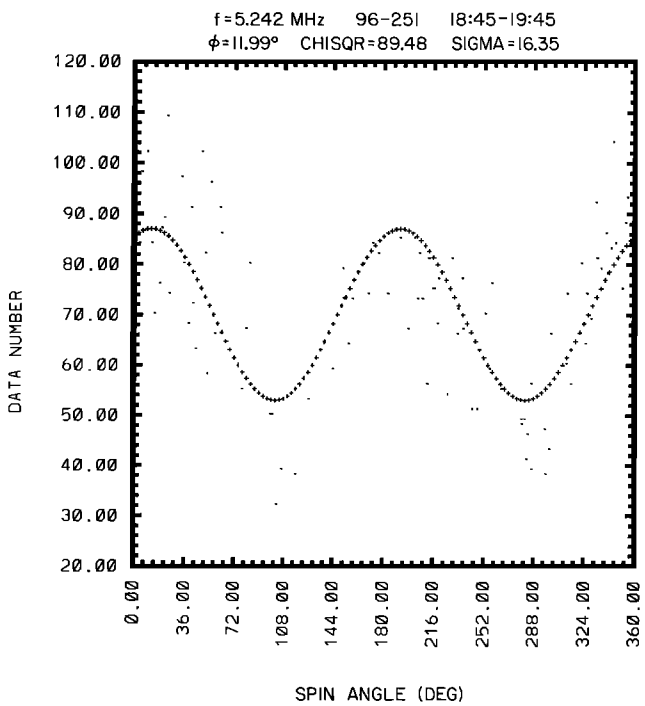

Figure 6a. Wave amplitude (data number) versus spin angle for $1845 < t < 1945$ on day 251 of 1996 at a frequency of 5.242 MHz.

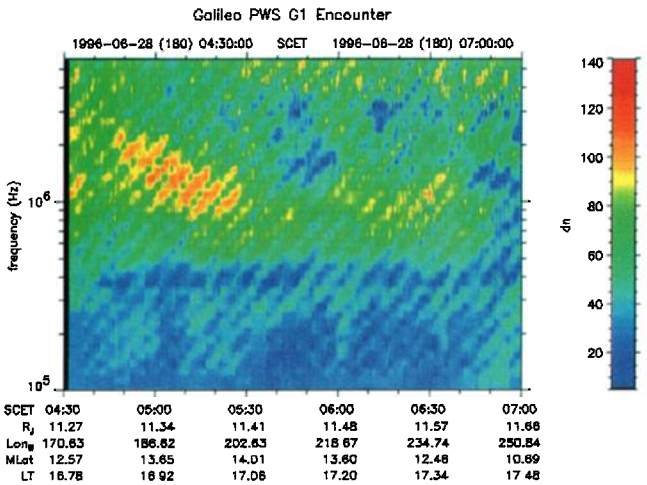

Plate 1. Frequency-versus-time spectrogram of PWS data for day 180 of 1996, just after the first Ganymede (G1) flyby. The spin modulation is seen after about 0430 for frequencies $f > 100$ kHz.

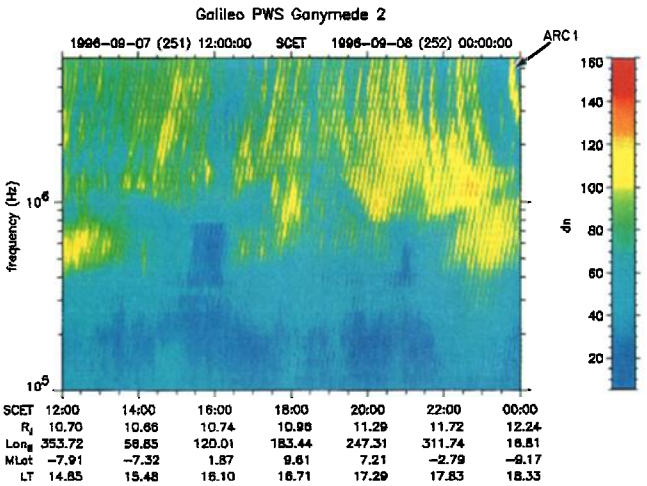

Plate 2a. Frequency-versus-time spectrogram of PWS data for day 251 of 1996 for times 1200–2400, just after the second Ganymede (G2) flyby. The spin modulation is seen throughout this plot. Low-frequency holes in the HOM emission are seen centered near 1550 and 2120. These holes are believed to be caused by the occulting Io torus as the spacecraft crosses the magnetic equator. There is an isolated vertex-early arc near the end of the plot in the frequency range 2.0 MHz $< f <$ 5.6 MHz.

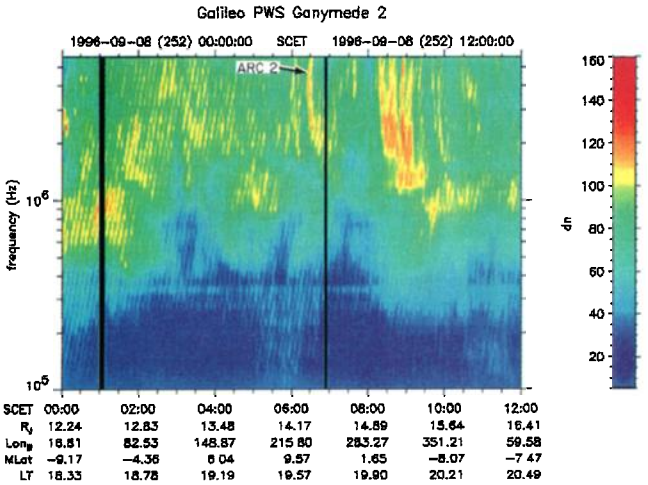

Plate 2b. Frequency-versus-time spectrogram of PWS data for day 252 of 1996 for times 0000–1200. This plot shows continued spin modulation from Plate 2a. Note the low-frequency holes in the HOM emission probably caused by occultations of the Io torus. In addition, an isolated vertex-early arc is seen centered near 0630 in the frequency range 2.0 MHz $< f <$ 5.6 MHz.

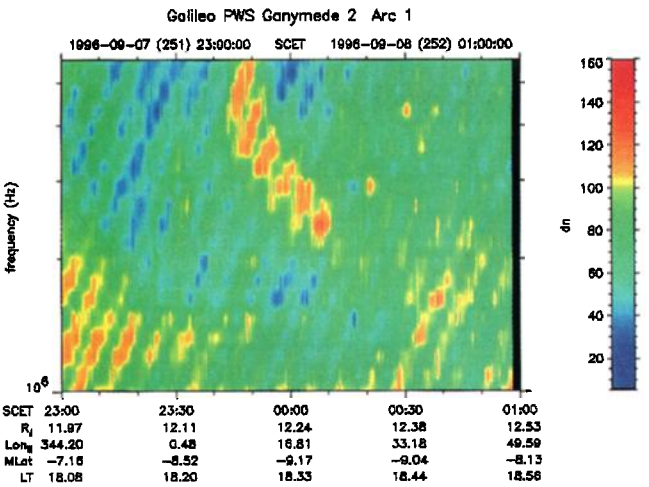

Plate 3a. High-resolution frequency-versus-time spectrogram of PWS data showing arc 1, which extends from about 2340 on day 251 to perhaps 0025 on day 252.

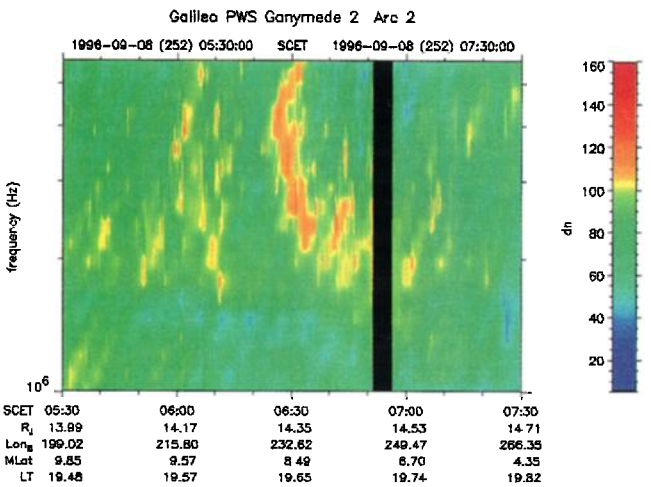

Plate 3b. High-resolution frequency-versus-time spectrogram of PWS data showing arc 2, which extends from about 0620 to about 0640 on day 252.

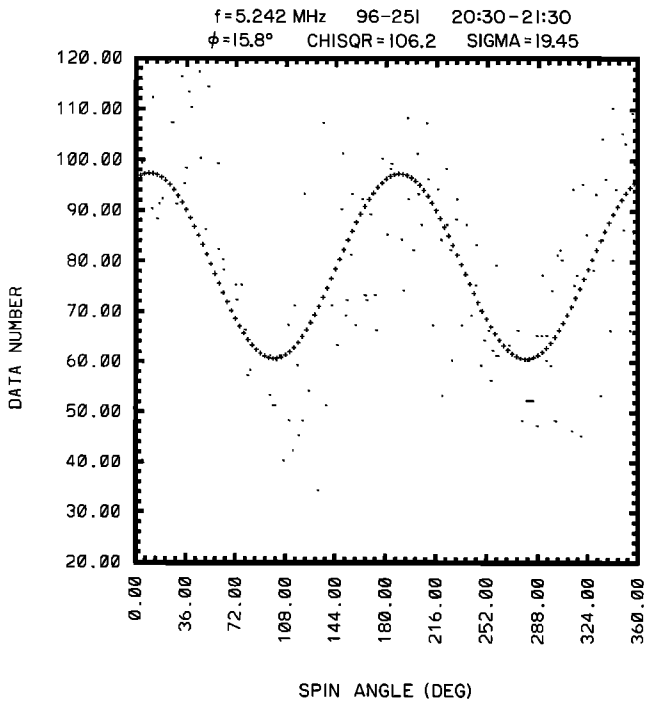

Figure 6b. Wave amplitude (data number) versus spin phase for $2030 < t < 2130$ on day 251 of 1996 at a frequency of 5.242 MHz.

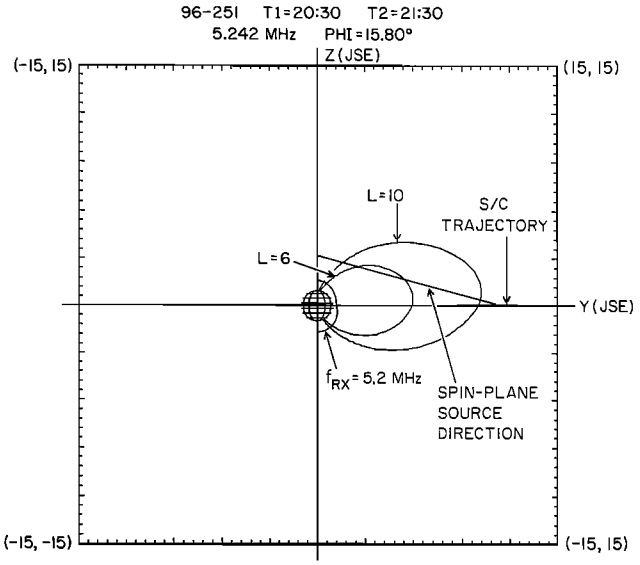

Figure 7b. Direction to the apparent source region projected into the JSE y-z plane. The direction is determined from the data of Figure 6b.

3.2. HOM/DAM Arcs

In the time interval 2340 on day 251 and extending to about 0020 on day 252, we observe an arc-like signature in the frequency range $f \geq 2.0$ MHz. We refer to this as arc 1 (Plate 2a). We believe this is a low-frequency extension of a decametric arc such as those so extensively studied from the Voyager data [cf. *Carr et al.*, 1983]. A similar signature (arc 2) is observed in the time interval 0610 to 0640 on day 252 as seen in Plate 2b. We have analyzed these signatures specifically, limiting the data to the times of the arcs only. This unfortunately severely limits the data, thus increasing the statistical errors of the analysis. We first analyze the data from each arc over the complete frequency range; then we examine the arcs separately for the higher and lower frequency range. In Plates 3a and 3b we show a high-resolution frequency-time spectrogram of arc 1 and arc 2, respectively. These arcs appear rather isolated as "vertex-early" arcs that apparently extend to higher frequencies. Arc 1 was observed when the spacecraft was located at magnetic latitude $\Lambda = -9°$ and at a system III longitude, $\lambda_{III} \sim 15°$. In contrast, arc 2 was observed when the spacecraft was located at $\Lambda = +8.5°$ and $\lambda_{III} = 235°$. In Figure 8 we plot the locations of the spacecraft and Io during the times of observation of arc 1 and arc 2. According to standard terminology, arc 1 could be classified as Io-C, except that it is vertex-early

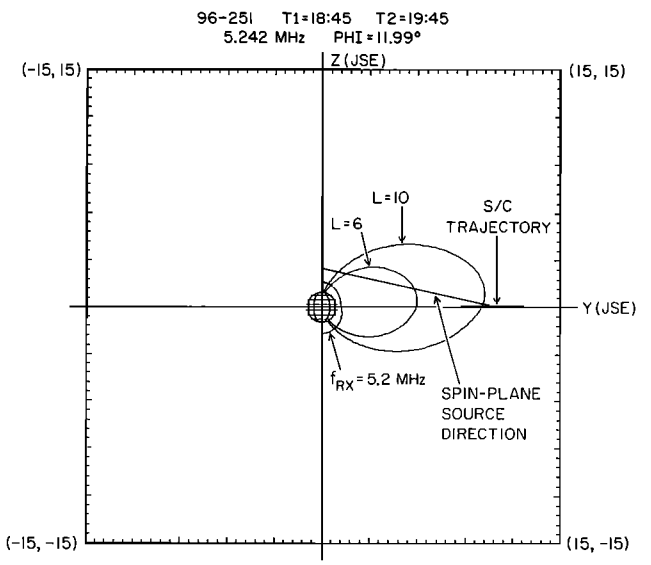

Figure 7a. Direction to the apparent source region projected into the JSE y-z plane. The direction is determined from the data of Figure 6a.

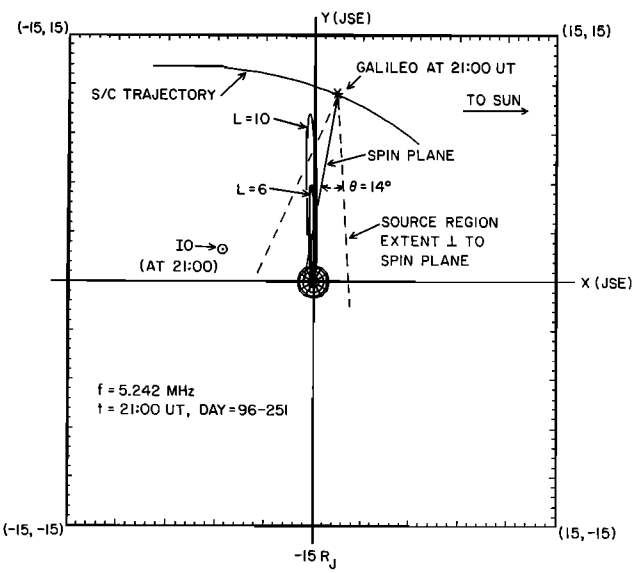

Figure 7c. Same as Figure 4b except for $t = 2100$ UT of day 96/251.

instead of vertex-late. Arc 2 cannot be classified as Io-A, Io-B, or Io-C because the orbital phase of Io relative to superior conjunction with the spacecraft is greater than 300° (cf. *Carr et al.* [1983] for a description of the Io-dependent sources). It is interesting to note that Ganymede is at ~90° from superior conjunction relative to Galileo for both arcs 1 and 2. This is consistent with the observation of vertex-early arcs if the source was the Ganymede flux tube [cf. *Kurth et al.*, 1997].

In Figure 9a we have plotted the arc 1 data number versus phase angle for 12 frequency channels in the range 2.0 MHz < f < 5.6 MHz. We estimate the statistical error of the fit to be about ±6°. The fit indicates an apparent source region in the spin plane of the satellite that is about 18° north of Jupiter. From the modulation index, we estimate the source region extent perpendicular to the spin plane to be $\theta < 22°$ measured in the JSE x-y plane. Gyroresonant sources would be expected to extend from about 1.5 R_J to nearly 2.5 R_J in this frequency range. We have therefore also fit the data for only the highest five frequency channels in the range 4.0 MHz < f < 5.6 MHz, as shown in Figure 9a, and then separately in the lower seven frequency channels, 2.0 MHz < f < 3.6 MHz. Somewhat surprisingly (but most probably due to the larger statistical error), the fit for the highest frequencies indicates an apparent source region to the north of Jupiter by the same angle, ~18°, with an error of approximately ±10°. In Figure 9c we plot the data for the lower frequency range with a fit indicating an apparent source region north of Jupiter by ~13° with an estimated error of ±9°. This latter location is more consistent with a gyroresonant source location as indicated in Figure 10, which shows the apparent spin-plane source directions projected into the JSE y-z plane for the higher and lower frequency range. Including more points in the fit as in Figure 9a lowers the statistical error, but we expect that the actual source regions are extended along an active magnetic field line.

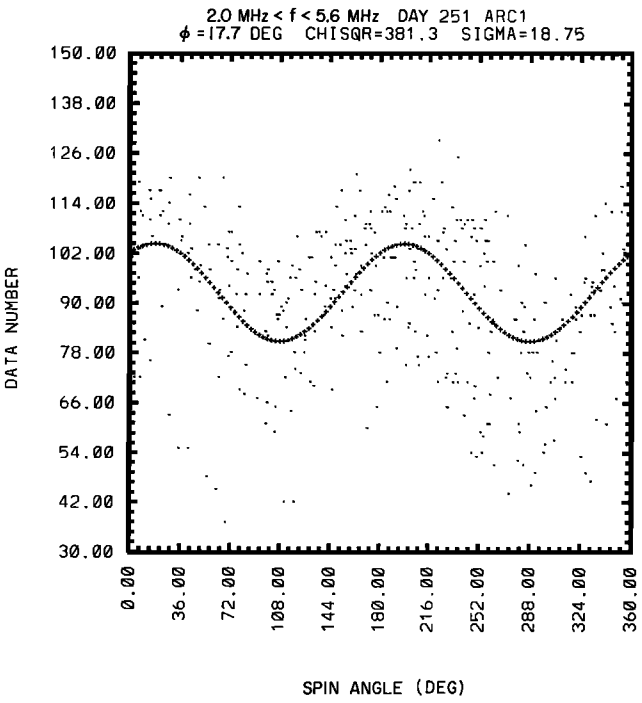

Figure 9a. Wave amplitude (data number) versus spin phase for arc 1, which was observed on day 251/252 from 2339 < t < 0023 in the frequency range 2.0 MHz < f < 5.6 MHz.

We have repeated the procedure for arc 2. In Figures 11a, 11b, and 11c, we plot the data points for fits to the respective frequency ranges 1.8 MHz < f < 5.6 MHz, 4.0 MHz < f < 5.6 MHz, and 1.8 MHz < f < 3.6 MHz. For this arc the apparent

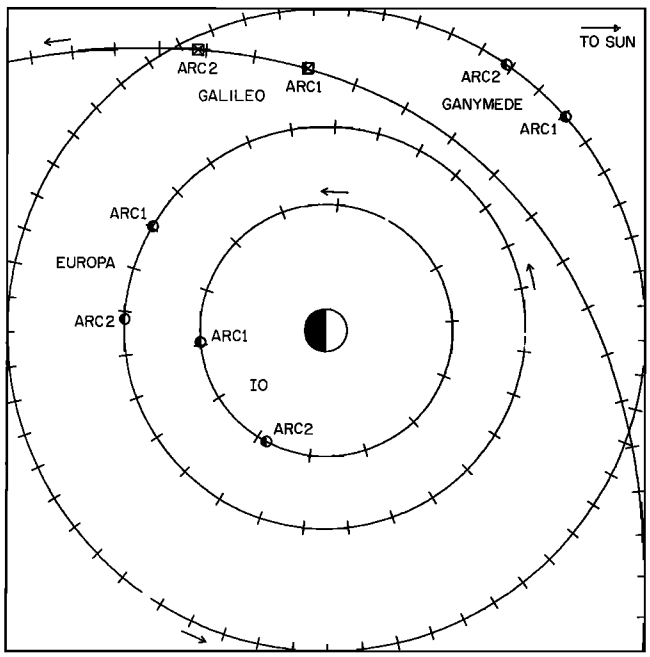

Figure 8. Two-dimensional trajectory of Galileo and orbital positions of the Jovian satellites at the observation times of arc 1 and arc 2 (tick marks are 3 hours apart).

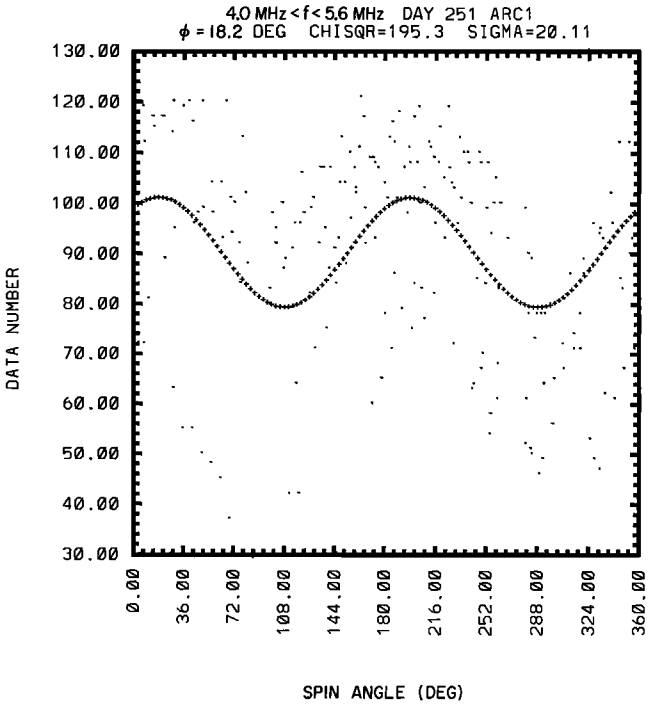

Figure 9b. Wave amplitude (data number) versus spin phase for arc 1 but now in the limited, higher frequency range 4.0 MHz < f < 5.6 MHz.

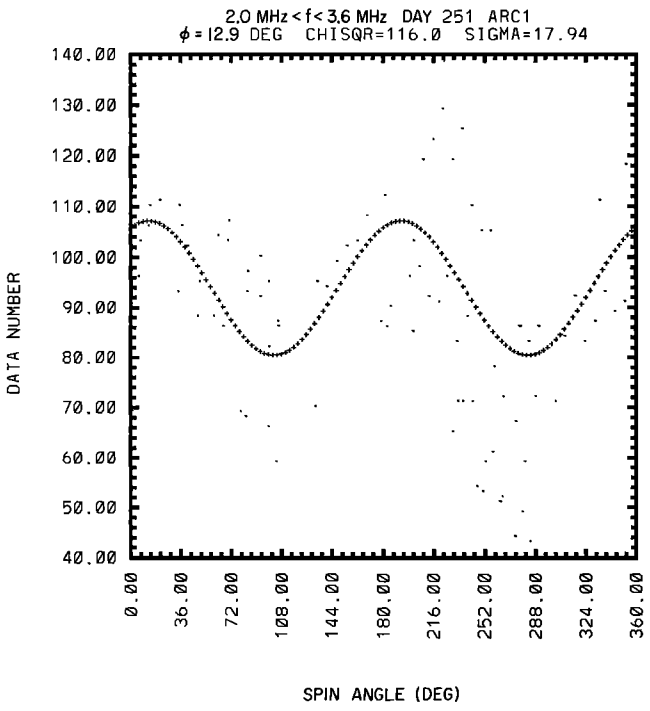

Figure 9c. Wave amplitude (data number) versus spin phase for arc 1 but now in the limited, lower frequency range 2.0 MHz $< f <$ 3.6 MHz.

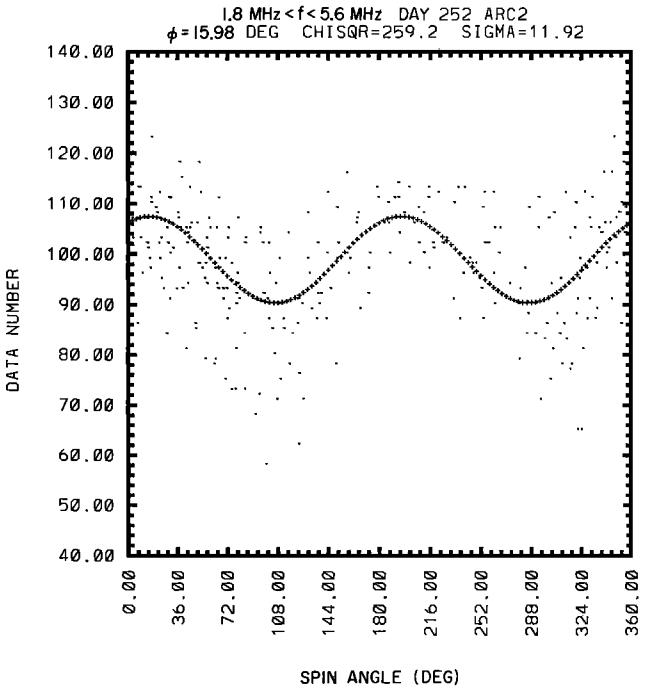

Figure 11a. Wave amplitude (data number) versus spin phase for arc 2, which was observed on day 252 from 0621 $< t <$ 0649 in the frequency range 1.8 MHz $< f <$ 5.6 MHz.

source region and estimated statistical error indicated by each plot is north of Jupiter by ~16 ± 6° (Figure 11a), ~9.5 ± 9° (Figure 11b), and 21 ± 8.5° (Figure 11c). From the modulation index for Figure 11a, we estimate the source region extent perpendicular to the spin plane to be $\theta < 17°$ measured in the JSE x-y plane. For the high- and low-frequency ranges the spin-plane directions to the apparent source region of arc 2 projected into the JSE y-z plane are shown in Figure 12. The fits to the data for arc 1 and arc 2 are summarized in Table 1. It is interesting to note that the apparent source regions are consistently north of Jupiter and higher than expected for a gyroresonant source, although the statistical errors do allow for such a source region. The statistical errors for the data of Figures 9 and 11 are large because the limited time extent of the arcs does not allow sufficient data accumulation.

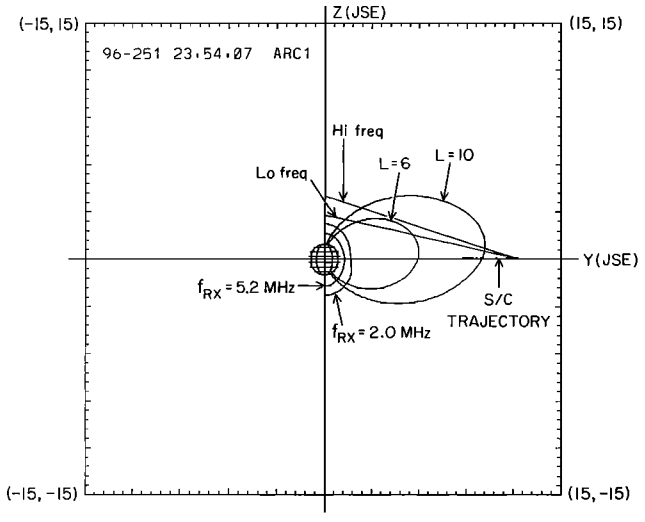

Figure 10. Directions to the apparent source region of arc 1 projected into the JSE y-z plane. The directions are determined from the data of Figures 9b and 9c.

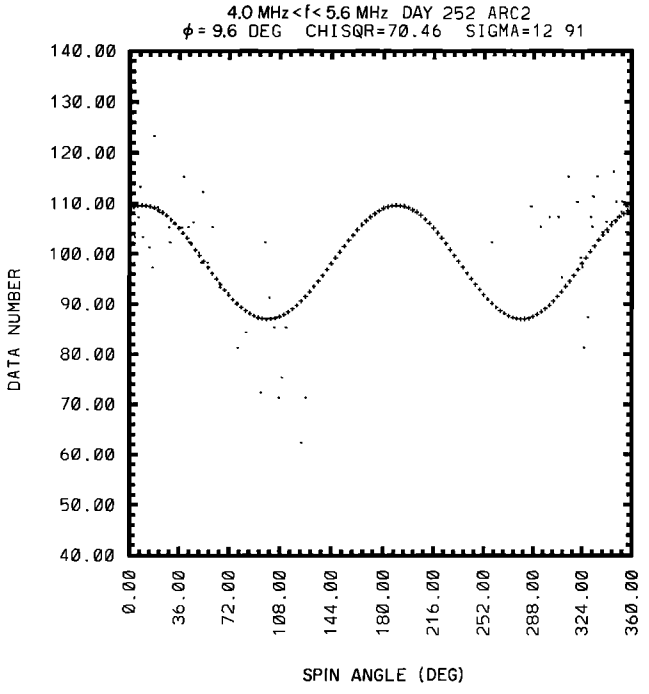

Figure 11b. Wave amplitude (data number) versus spin phase for arc 2 but now in the limited, higher frequency range 4.0 MHz $< f <$ 5.6 MHz.

4. Summary and Conclusions

The Galileo PWS instrument can be used to determine the spin-plane direction to apparent radio emission sources in the Jovian environment. Uncertainties associated with some of the analyses make it difficult to make definitive statements. In this paper we have considered only HOM/DAM emission, which is observed with frequent intensity amplifications or bursts that last typically for tens of minutes and are separated from each other by somewhat larger periods of time. Each period of intensity amplification may have a different source region from the lower intensity, have a more ubiquitous emission, or come from other bursts of emission. HOM/DAM arcs, which apparently are low-frequency extensions of DAM arcs, are also observed occasionally as enhanced emission superimposed on a lower intensity background. Both the Io and Ganymede flux tubes are possible source regions of the arc signatures, but only Ganymede has the expected orbital phase for the vertex-early arc curvature. The more ubiquitous continuous emission, bursts, and the HOM/DAM arcs all appear to propagate from high latitudes of Jupiter, consistent with gyroresonant source regions. Some statistically meaningful events, however, appear to have a source region that is at a lower or higher altitude than required for a gyroresonant source (day 180, Figure 4a and day 251, Figure 7b, for instance). Such events may be the result of large Io torus refraction (perhaps resulting from asymmetries in the torus) or may come from source regions requiring an alternative free-energy source such as electron beams.

Figure 4a indicates a statistically meaningful apparent source region at an altitude that is lower than expected for a gyroresonant source. This result is consistent, however, with ray refraction of HOM emission that focuses rays into the equatorial region. This is due to large plasma density in the Io torus that falls off with distance away from the magnetic equatorial plane, as clearly indicated by the results of *Ladreiter et al.* [1994] and *Wang* [1994]. At frequencies <1 MHz, wave refraction of over 10° is possible due to the Io torus, and could easily explain the apparent source region of Figure 4a [cf. *Ladreiter and Lablanc*, 1990, Figures 6 and 7, pp. 6429 and 6430, respectively; also *Wang*, 1994]. However, our results show that sometimes, even at higher frequencies, radio emission appears to come from source regions at altitudes above a gyroresonant source region (see Figure 7b). This is difficult to explain by refraction unless asymmetries in the Io torus density exist, with density increasing away from the magnetic equator. These asymmetries might take the form of enhanced density islands which occasionally occur along magnetic field lines.

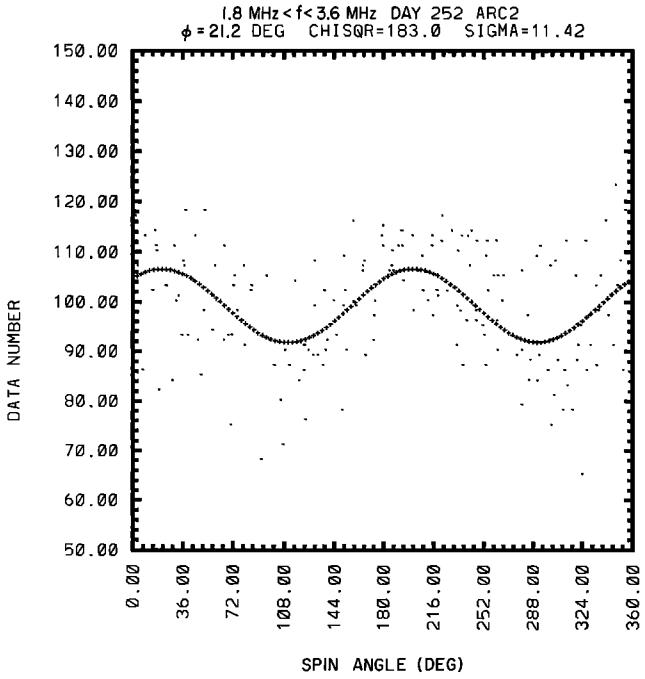

Figure 11c. Wave amplitude (data number) versus spin phase for arc 2 but now in the limited, lower frequency range 1.8 MHz $< f <$ 3.6 MHz.

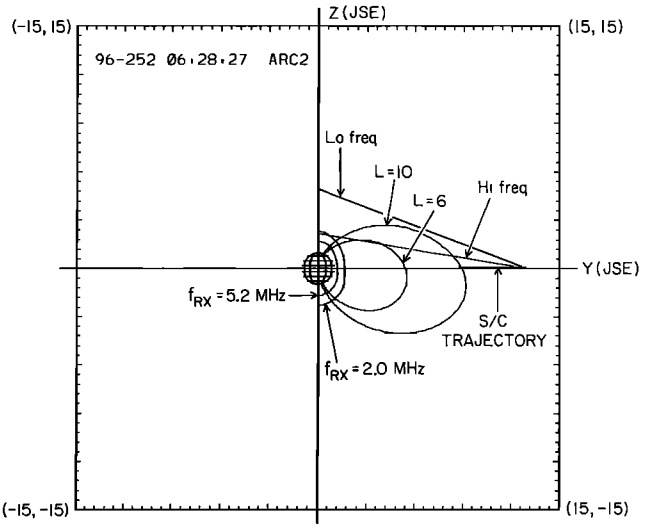

Figure 12. Directions to the apparent source region projected into the JSE y-z plane for arc 2 for the high-frequency (4.0 MHz $< f <$ 5.6 MHz) and the low-frequency (1.8 MHz $< f <$ 3.6 MHz) range.

We note that ray paths probably intercept dense parts of the Io plasma torus, which is now believed to contain many azimuthal and latitudinal asymmetries [cf. *Schneider et al.*, 1997; *Desch et al.*, 1994; *Thomas and Lichtenberg*, 1997]. The density of the torus in the region of Io has been observed by Galileo, and it is reported to be as large as 5300 cm^{-3} (about twice the density observed during the Voyager flyby) with a peak of about 41,000 cm^{-3} in the Io wake [cf. *Gurnett et al.*, 1996]. *Menietti and Reiner* [1996] have shown that even for observers at high latitude, the Io torus is capable of refracting emission out of the meridian plane, for instance. If, however, the emission source is actually at high latitudes, above the gyroresonant source region (for example, the event shown in Figure 7b),

Table 1. Summary of Results for Arc 1 and Arc 2

Δf, MHz	Spin Angle 0° = Jupiter	Statistical Error, deg
	Arc 1	
2.0–5.6	18°N	±6
2.0–3.6	13°N	±9
4.0–5.6	18°N	±10
	Arc 2	
1.8–5.6	16°N	±6
1.8–3.6	21°N	±8.5
4.0–5.6	9.5°N	±9

then it would be necessary to postulate an alternative free-energy source for wave generation for these events. One possible alternative emission mechanism is the temperature anisotropic beam constability [*Wong and Goldstein*, 1990; *Winglee et al.*, 1992], which requires electron beams and a plasma distribution with an electron temperature anisotropy ($T_\perp/T_\parallel > 1$). Electron beams have been observed near Io [*Williams et al.*, 1996]. It is not known, however, if the required temperature anisotropies for electrons exist outside of the Io torus. Such a mechanism would allow wave generation at frequencies less than the local gyrofrequency by an amount dependent upon the energy of the electron beams.

Acknowledgments. We wish to thank K. Kurth for typing the manuscript. This work was supported by NASA grant 958779 with the Jet Propulsion Laboratory.

References

Carr, T. D., M. D. Desch, and J. K. Alexander, Phenomenology of magnetospheric radio emissions, in *Physics of the Jovian Magnetosphere*, edited by A. J. Dessler, pp. 226–284, Cambridge Univ. Press, New York, 1983.

Desch, M. D., W. M. Farrell, and M. L. Kaiser, Asymmetries in the Io plasma torus, *J. Geophys. Res.*, *99*, 17,205, 1994.

Fainberg, J., L. G. Evans, and R. G. Stone, Radio tracking of energetic particles through interplanetary space, *Science*, *178*, 743, 1972.

Gurnett, D. A., W. S. Kurth, R. R. Shaw, A. Roux, R. Gerdrin, C. F. Kennel, F. L. Scarf, and S. D. Shawhan, The Galileo plasma wave investigation, *Space Sci. Rev.*, *60*, 341, 1992.

Gurnett, D. A., W. S. Kurth, A. Roux, S. J. Bolton, and C. F. Kennel, Galileo plasma wave observations in the Io plasma torus and near Io, *Science*, *274*, 391, 1996.

Kurth, W. S., M. M. Baumback, and D. A. Gurnett, Direction finding measurements of auroral kilometric radiation, *J. Geophys. Res.*, *80*, 2764, 1975.

Kurth, W. S., S. J. Bolton, D. A. Gurnett, and S. Levin, A determination of Jovian hectometric radiation via occultation by Ganymede, *Geophys. Res. Lett.*, *24*, 1171, 1997.

Ladreiter, H. P., and Y. Leblanc, Source location of the Jovian hectometric radiation via ray-tracing technique, *J. Geophys. Res.*, *95*, 6423, 1990.

Ladreiter, H. P., and Y. Leblanc, The Jovian hectometric radiation: An overview after the Voyager mission, *Ann. Geophys.*, *9*, 784, 1991.

Ladreiter, H. P., P. Zarka, and A. Lecacheux, Direction finding study of Jovian hectometric and broadband kilometric radio emissions: Evidence for their auroral origin, *Planet. Space Sci.*, *42*, 919, 1994.

Menietti, J. D., and M. J. Reiner, Modeling of Jovian hectometric radiation source locations: Ulysses observations, *J. Geophys. Res.*, *101*, 27,045, 1996.

Menietti, J. D., D. A. Gurnett, W. S. Kurth, J. B. Groene, and L. J. Granroth, Radio emissions observed by Galileo near Io, *Geophys. Res. Lett.*, *25*, 25–28, 1998.

Morgan, D. D., and D. A. Gurnett, The source location and beaming of terrestrial continuum radiation, *J. Geophys. Res.*, *96*, 9595, 1991.

Reiner, M. J., J. Fainberg, and R. G. Stone, Source characteristics and locations of hectometric radio emissions from the northern Jovian hemisphere, *Geophys. Res. Lett.*, *20*, 321, 1993a.

Reiner, M. J., J. Fainberg, and R. G. Stone, Source characteristics of Jovian hectometric radio emissions, *J. Geophys. Res.*, *98*, 18,767, 1993b.

Reiner, M. J., M. D. Desch, M. L. Kaiser, R. Manning, J. Fainberg, and R. G. Stone, Elliptically polarized bursty radio emissions from Jupiter, *Geophys. Res. Lett.*, *22*, 345, 1995.

Schneider, N. M., M. H. Taylor, F. J. Crary, and J. T. Trauger, On the nature of the λ_{III} brightness asymmetry in the Io torus, *J. Geophys. Res.*, *102*, 19,823, 1997.

Thomas, N., and G. Lichtenberg, The latitudinal dependence of ion temperature in the Io plasma torus, *Geophys. Res. Lett.*, *24*, 1175, 1997.

Wang, L., Investigation of hectometric and kilometric radio emissions from Jupiter and Neptune, Ph.D. dissertation, Univ. of Fla., Gainesville, 1994.

Williams, D. J., et al., Electron beams and ion composition measured at Io and in its torus, *Science*, *274*, 401, 1996.

Winglee, R. M., J. D. Menietti, and H. K. Wong, Numerical simulations of bursty radio emissions from planetary magnetospheres, *J. Geophys. Res.*, *97*, 17,131, 1992.

Wong, H. K., and M. L. Goldstein, A mechanism for bursty radio emission in planetary magnetospheres, *Geophys. Res. Lett.*, *17*, 2229, 1990.

L. J. Granroth, J. B. Groene, D. A. Gurnett, W. S. Kurth, and J. D. Menietti, Department of Physics and Astronomy, University of Iowa, 203 Van Allen Hall, Iowa City, IA 52242-1479. (e-mail: jdm@space.physics.uiowa.edu)

(Received August 1, 1997; revised October 28, 1997; accepted December 1, 1997.)